5-6-2011

Recording of Elevated Temperature Fatigue Crack Growth Data by DCPD System

N. Ramachandran

N. Arakere

Tarun Goswami
Wright State University - Main Campus, tarun.goswami@wright.edu

Recording of Elevated Temperature Fatigue Crack Growth Data by DCPD System

N. Ramachandran[1], N. Arakere[2] and T. Goswami[1]

[1]*Damage Tolerance Group (MS 9/Dept. 178), Cessna Aircraft Company, One Cessna Blvd, Wichita, KS 67215, USA;*
[2]*Associate Professor, Mechanical Engineering Department, University of Florida, Gainsville, FL 32611, USA*
[1]*Adj. Associate Professor, Department of Mechanical Engineering, Wichita State University, Wichita, KS 67250-0035, USA*

ABSTRACT

The growth of "long" fatigue cracks, in α–β titanium alloy forging, subjected to cyclic stresses, is studied in this paper. The fatigue crack growth rate (FCGR) data were recorded at room temperature, 350, 450, 550 and 650°F using the Direct Current Potential Difference (DCPD) technique. The DCPD method, used in this investigation, was found to record and correlate the potential difference in terms of crack growth rate (da/dN) and Mode I stress intensity factor range satisfactorily. Various factors related to error minimization and calibration equations for compact tension specimens have been elaborated. Also discussed were the means to enhance the accuracy of the data by the DCPD system for elevated temperature fatigue crack growth rate testing.

INTRODUCTION

Most metallic materials, in general, contain a distribution of microscopic cracks throughout the material. Therefore, materials are not homogeneous, isotropic and defect free. It is therefore of practical importance to study the growth of cracks in materials that are subjected to cyclic stresses, in order to estimate the service life of components. The damage tolerant (DT) based methodologies are the subject of increased interest throughout the gas turbine engine community to establish life limits of various rotating/non-rotating components. The basis for DT based methods is to assume the presence of cracks at sites of potential stress concentrations arising from design requirements of a disk-blade-shaft assembly. Following crack detection, the crack is presumed to grow at a rate predicted by Linear Elastic Fracture Mechanics (LEFM) or other methods until it reaches a critical size, beyond which catastrophic failure of the component occurs.

The crack growth rates and size parameters are established analytically based on approximation of service loads and other operating conditions. Such data may enable the computation of the time between the component replacement and to establish a Safe Inspection Interval (SII).

Since FCG is a complex interaction of stress, environment and microstructure of materials, analytical estimation of FCGR is very difficult as characteristics like microstructure, temperature, etc., cannot be incorporated in a material model effectively. Hence, experimental evaluation of FCGR properties is essential, since such experimental data would enhance the reliability of analytical methods.

It is therefore of practical importance that growth of cracks in materials subjected to cyclic stresses is studied in detail, which will enable life prediction of components. Large rotating components in aircraft gas turbine engines are the most critical structural components and their integrity is vital to the safety of the aircraft. The demand for increased performance in aircraft engines reflects on improvements in operating temperatures and stresses, which in turn result in accelerated fatigue damage.

The objective of this research is to determine fatigue crack growth rate data for Ti-6Al-4V forging specimens in a range of temperatures from room temperature to 650°F using the Direct Current Potential Drop (DCPD) method. The compact tension (CT) specimens

were tested in the long crack regime that simulate typically a two dimensional through the thickness crack scenario. The configuration of a CT specimen that could be cut from an engine compressor disc is shown in Fig. 1. In a rotating disk, centrifugal stresses induced due to rotation ranges maximum at the inner diameter, called the bore, and vary through the radius. Such stresses tend to open a crack that may have formed at the inner diameter, causing it to grow radially outwards. Hence, a CT specimen simulates the behavior of a crack under such loading conditions and data obtained from such tests will reveal FCGR closer to the operating conditions.

The parameters that control crack growth rate (da/dN versus ΔK) can be used in DT procedures, for determining the safe operating life. A typical da/dN vs ΔK plot has three regions of fatigue crack growth, shown in Fig. 2. Region I, in which growth of "short or

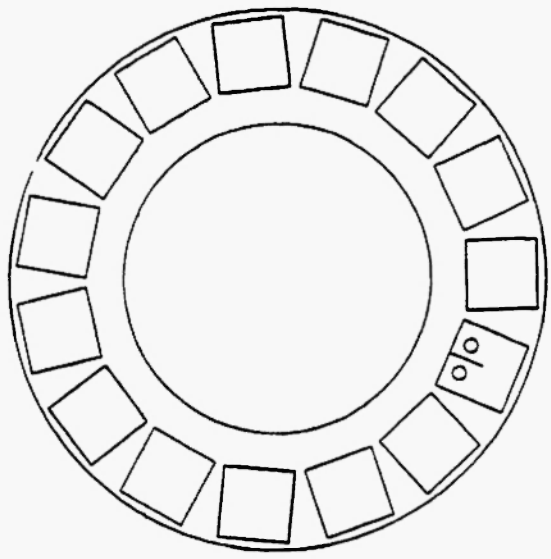

Fig. 1: Orientation of the C(T) specimen in the disk.

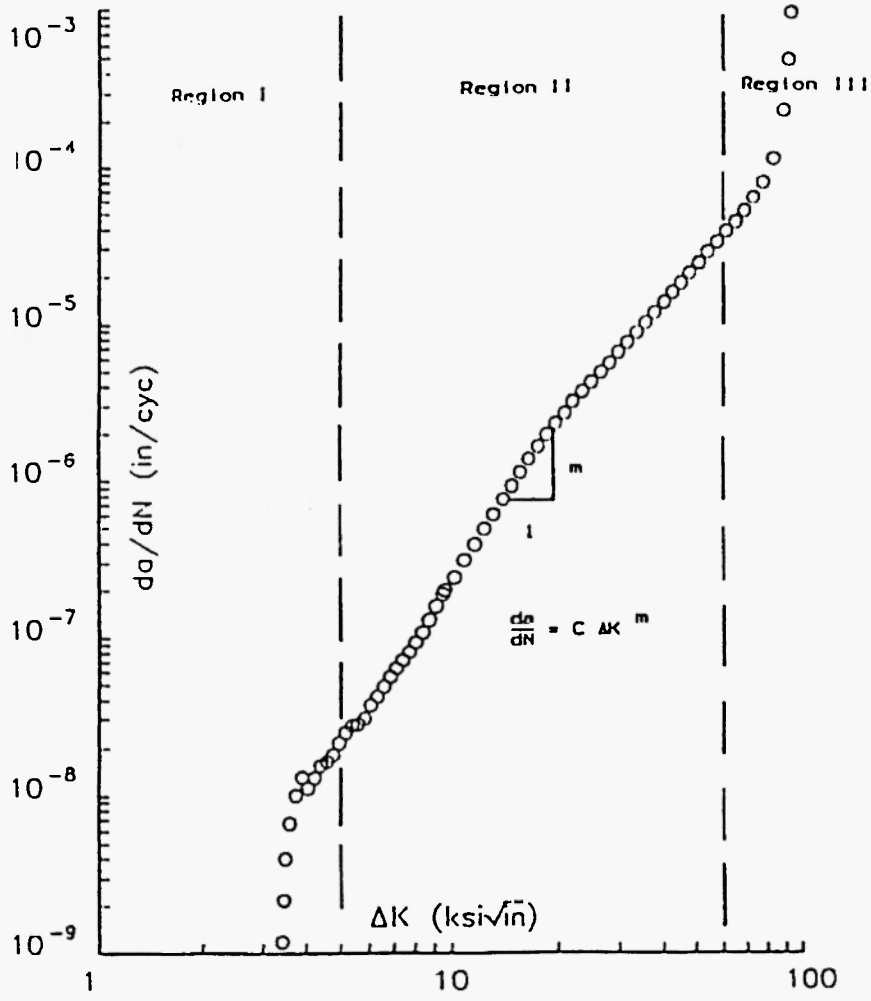

Fig. 2: Typical Da/Dn vs. ΔK plot showing three regions of behavior.

small" cracks occurs, is beyond the scope of this paper. Region II is essentially the region of interest for design purposes since it represent stable crack growth and is the linear region in which general material models can be developed. Region III relates to unstable crack growth, which culminates in failure. The DCPD method, used in this study, records the FCGR data corresponding to Region II.

TITANIUM ALLOYS

Titanium and titanium alloys are noted primarily for their outstanding strength to weight ratios, elevated temperature properties, corrosion resistance, excellent metallurgical stability, good fatigue properties and raw material availability combined with fabrication properties. Owing to these properties, titanium and titanium alloys are extensively used in aircraft, marine, processing equipment industry, space technology, and also in defense technology applications.

Titanium and titanium alloys are classified into three major categories according to the predominant phase in the microstructure. Titanium has a closed packed hexagonal structure called alpha phase at room temperature. At approximately 1625°F the alpha phase transforms to a Body Centered Cubic (BCC) structure called beta phase which is stable up to the melting point of 3000–3100°F. Aluminum together with carbon, oxygen and nitrogen stabilize the alpha phase and raise the α–β transformation temperatures. Beta stabilizers include copper, chromium, iron, manganese, molybdenum, tantalum and vanadium. Alpha alloys are weldable, non heat treatable up to 1000°F, strong at cryogenic temperatures, more oxidation resistant than beta or α–β alloys and are relatively more difficult to form. Beta alloys are weldable, heat treatable, stable up to about 600°F, strong at higher temperatures for short periods, and are quite formable at room temperature. The α–β alloys are heat treatable, stable up to 800°F, strong, more formable than alpha alloys and are more difficult to weld. This group contains the largest number of commercial alloys. The alloys are formulated such that both the hexagonal alpha phase and the BCC beta phase co-exist at room temperature. A wide range of properties can be obtained in this group owing to their response to heat treatment that alters both the phase compositions and also the quantity of the alpha and beta phases.

Titanium alloys are available in wrought, cast and also powder metallurgy forms, where wrought form accounts for 95% of the market. The properties of these forms will vary depending on their interstitial contents and thermal-mechanical processing. The driving force for the development of high temperature titanium alloys has been the gas turbine, with widespread inclusion of the alloy in engine design since the early 1950s. Many titanium alloys have been launched to match specific targets linked with major engine programs, and the development of titanium alloys parallels the advances made in engine performances over the same period. The titanium alloys C Ti-70, Ti 5-2.5, T 6-4, Ti 6-6-2, and Ti 6-2-4-2 are predominantly used in jet engines.

The FCGR data for Ti-6Al-4V alloy forging were reported by many workers, for example /1-6/, and FCGR were recorded by the DCPD system /7-16/. Raizenne /10/ used compact tension specimens and the direct current potential drop method to record the CGR data. In this AGARD effort, tests were conducted with stress ratios of 0.1 and 0.7 along with simple and complex loading sequences. Fatigue crack growth behavior of Ti-6Al-4V at elevated temperatures in high vacuum has been reported in the literature /5/. The near threshold crack propagation in Ti-6Al-4V was studied at room temperature and 572°F in air. The specific influence of air environment was studied by comparing the crack propagation behavior at room temperature and also at 572°F. A detrimental environmental effect on propagation rates below 10^{-8} m/cycle resulting in accelerated FCG has been reported. This report also indicates an increase in FCGR at higher temperatures that could be attributed to a reduction of the Young's modulus with increasing temperature. Fatigue crack growth in Ti-6Al-4V at elevated temperatures has been reported in /4,10/. Tests were conducted at 392, 752 and 932°F where crack growth rates were higher at higher temperatures than at room temperature.

Several methods were utilized to record the FCGR data that may be summarized as: optical, compliance, crack gauges, acoustic emission, and electrical potential difference method. However, at elevated temperatures, oxides develop and fill the specimen surface and make

determination of actual crack tip a difficult process. Also, tests must be interrupted numerous times in order to measure the crack growth through the specimens. Therefore, in this investigation, an automated computer recording of the FCGR was developed through the DCPD system.

DIRECT CURRENT POTENTIAL DROP (DCPD) METHOD

The standard method of determining fatigue crack growth rate (FCGR) involves application of cyclic loading to a specimen which has been pre-cracked by fatigue and the crack length is measured by visual or by other equivalent methods as a function of elapsed cycles. The rate of crack growth can be determined by analysis of test data and crack growth rates da/dN can be determined based on ΔK, using LEFM methods as described earlier. Hence, this data characterizes materials' resistance to stable crack growth under cyclic loading and can be utilized for design and life predictions of engineering structures.

In general, any method that can measure displacements or stress can be used to establish fatigue crack growth characteristics of a material. The measurement of stresses or displacements will enable estimation of fatigue crack growth rates by substituting them in closed form expressions if available or by other analytical methods. Conventional methods of measuring fatigue crack growth are the visual methods and the automated methods. Visual techniques are generally based on the monitoring of crack growth using marker bands on the surface of the specimen and successive crack lengths are recorded either using an optical microscope or a camera to photograph the crack tip at regular intervals. There are a few other visual techniques that are minor variations of the methods mentioned earlier.

Traditional methods for monitoring crack growth involve visual monitoring of crack growth which is quite unreliable, inadequate and also very often uneconomical. The two most common techniques used are the compliance and the electric potential techniques. The compliance method involves measurement of the crack tip opening displacement to establish a relationship between the load and the crack length. The electrical potential drop method on the other hand is based on detection of the change in electrical potential of a specimen with change in crack length. These methods, although simple in concept, require sensitive instrumentation and detailed planning. The non-visual techniques essentially provide data that have very little scatter and are more reliable, especially in extended testing conditions where continuous monitoring of the tests is not feasible. Moreover, these methods are absolutely essential when testing is conducted at high temperatures or prohibitive environments. Automated methods provide for automation of testing beyond mere acquisition of crack growth data. This is with respect to control of loading rates and other parameters during testing in the threshold region which might be required to maintain consistent monitoring of very slow growth rates. Recent developments in the field of personal computer technology have facilitated the use of automated techniques with substantial cost savings. The various constituents of an automated test setup such as analog-digital converters, direct memory access, vectored input, digital waveform generators, control interfaces and high resolution graphics can be easily established in personal computers, thus making an automated test setup more easily affordable than software development costs for similar requirements.

FUNDAMENTAL PRINCIPLE

Establishing crack length from the DCPD method is based on the fact that the electric field in a cracked specimen with a constant current flowing through it is a function of specimen geometry and the crack length. If a constant current is maintained through the specimen, then the electric potential or the voltage drop across the crack plane will increase as the crack grows owing to modification of the electric field and the subsequent perturbation of the current field in the specimen. The change in voltage can be associated with corresponding crack lengths through analytical or experimental calibration relationship /11/. A general layout of the DCPD method is shown in Fig. 3. The DCPD method can be applied to all conducting materials and also insulators if a film of conducting

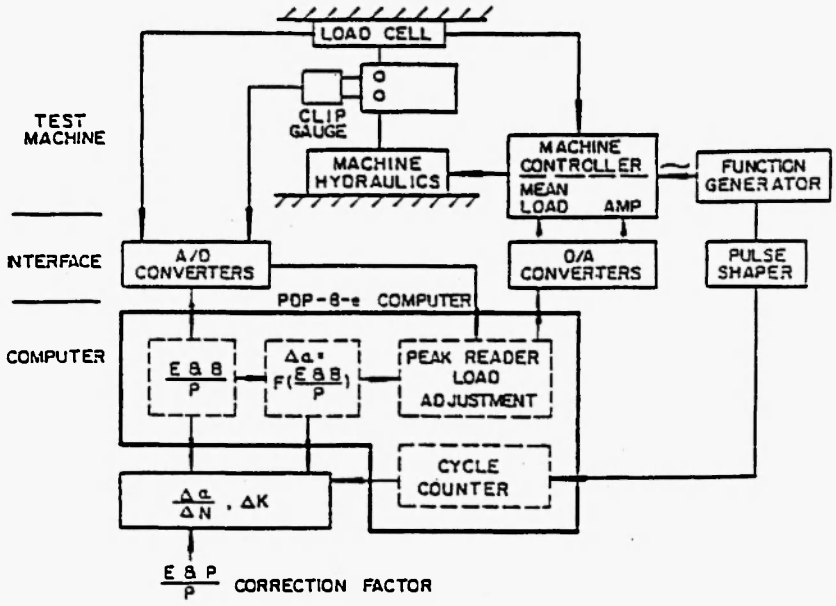

Fig. 3: General layout of an automated fatigue system.

material is attached to it. The voltages measured are in the 0.1-50 millivolt range with a precision of ± 0.1%. Special precautions should be taken to minimize electrical noise, thermally induced electromagnetic fields and instrumentation drift. Further, EPD measurements will also be susceptible to crack surface shorting, location of current, and potential leads, temperature, environment and dynamic loading effects.

CALIBRATION

Close form solutions relating the potential difference to crack length have been analytically derived for several standard specimen geometries such as the middle tension M(T), corner cracked (CC), compact tension (CT) and the part through surface crack specimens /11,14-16/. Such relationships are usually expressed in terms of the normalized voltage (V\V0) and a reference crack length (a) as follows:

$$a = f\left(\frac{V}{V_o}, a_o\right) \quad (1)$$

V is the measured voltage, V_o is the voltage corresponding to an initial or crack length, a is the crack length, and a_o is the crack length associated with V_o. Generally the non-dimensional term a\W (where W is specimen width) is expressed as a function of V\V_o. This provides a relationship that is independent of the material, specimen thickness and input current magnitude.

Sometimes the complexity and form of the solution requires that a look-up table containing values of V|V0 and a|W be generated. Such empirical relationships can often be advantageous in those instances where sample geometries are complex or where wire placement pertaining to an existing relationship must be altered. In any event, all such relationships should be experimentally verified using visual observations, either optical surface measurements or post-test fatigue surface measurement. The calibration constant a_o and V_o may be any crack length and corresponding EPD measurement where the crack length has been determined visually. Optical surface measurements may be used to determine a_o, provided crack front curvature is not significant or is not accounted for /7/. If real time crack measurement is not required during the test, post test fatigue surface measurement may be used to determine a_o /7/.

COMPACT TENSION SPECIMEN GEOMETRY

One example of the relationship between EPD and crack length for the (CT) sample geometry is shown in Eq. (2). Hicks and Packard used finite element analysis to develop one such relationship and verified through both analog and experimental techniques for a/W ratios ranging from 0.24 to 0.7 /14/.

$$\frac{V}{V_o} = 0.5766 + 1.9169 \bullet \left(\frac{a}{W}\right) - 1.0712 \bullet \left(\frac{a}{W}\right)^2 + 1.6898 \bullet \left(\frac{a}{W}\right)^3 \quad (2)$$

where a is the crack length, V is the measured potential, V_o is the initial potential corresponding to a\W = 0.241. The term accounts for the linearity and small changes in applied current, specimen dimensions, and associated errors arising from wire placement on sample to sample. In reverse notation Eq. (2) can be written as

$$\frac{a}{W} = 0.5051 - 0.8857 \bullet \left(\frac{V}{V_o}\right) - 0.1398 \bullet \left(\frac{V}{V_o}\right)^2 + 0.0002398 \bullet \left(\frac{V}{V_o}\right)^3 \quad (3)$$

The above equation has been employed in two international multi-laboratory cooperative testing efforts /3,10/. A typical compact tension specimen is shown in Fig. 4 and Fig. 5 which illustrates the specific wire placements for conducting the tests. The above mentioned relationship is valid only for the wire locations shown. These were determined by a compromise between sensitivity and reproducibility.

Aronson and Ritchie /15/ used finite element technique to determine the electric potential distribution in a standard CT specimen. Their study focused on the optimum location for input current and potential leads based on the accuracy, sensitivity, reproducivity, and measurability. These terms were defined and related with the data in the original reference. Other workers suggested that by slightly altering the optimum current and potential lead positions, Johnson's equation, originally developed for M(T) specimens, might be applicable to CT specimens. However, it should be recognized that good agreement between Johnson's equation for CT specimens and experimental results may not be universal for all ratios of EPD gage length to sample width. Pishva *et al.* /16/ developed similar equations for thin sheet specimens for elevated temperature tests for the extended CT specimens and

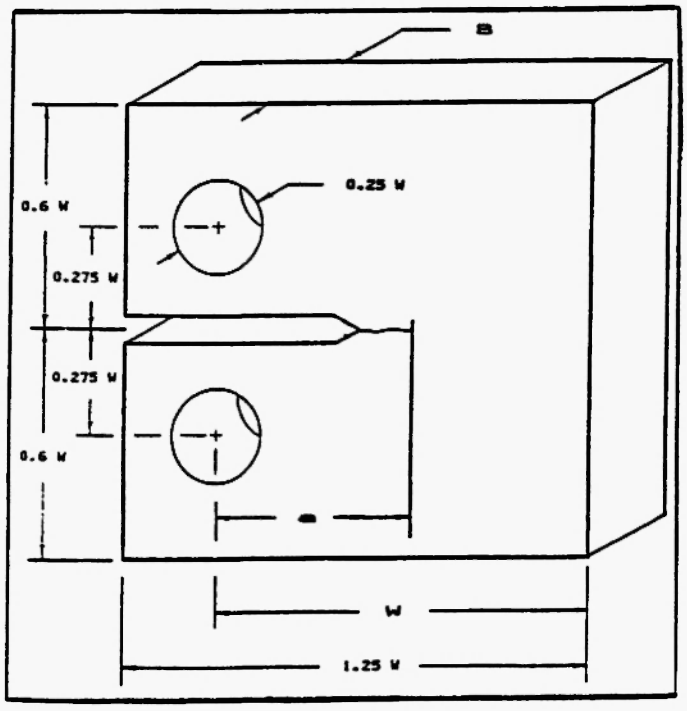

Fig. 4: Configuration of the C(T) specimen.

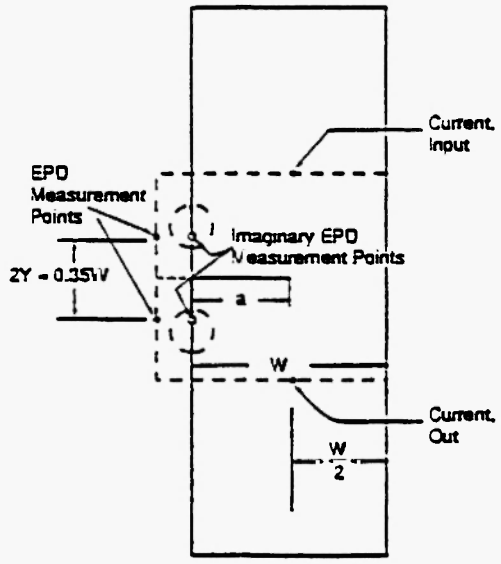

Fig. 5: Representation of the C(T) specimen using Johnson's formula.

the coefficients used by them were different.

METHODOLOGY FOR MEASURING CRACK GROWTH RATE

The variables: thickness (B), width (W), initial notch depth and load parameters, including maximum load (P_{max}), stress ratio (R) and the K gradient are to be used. An appropriate current and voltage level to be maintained across the specimen was selected. A relationship between the initial notch depth or the pre-crack length and the voltage across the crack tip is established by using Eq. (2) or Eq. (3), in the case of a CT specimen. Substitution of the initial or current a/W and the corresponding voltage V_o will yield the current voltage across the crack field. This voltage is used to determine the new crack length (a). The determination of a leads to the establishment of the SIF at the crack tip, using Eq. (4) below, in the case of a CT specimen.

$$K = \frac{P}{B \bullet W^{\frac{1}{2}}} \frac{\left(2 + \frac{a}{W}\right)}{\left(1 - \frac{a}{W}\right)^{\frac{3}{2}}} \left[0.886 + 4.64\left(\frac{a}{W}\right) - 13.32\left(\frac{a}{W}\right)^2 + 14.72\left(\frac{a}{W}\right)^3 - 5.6\left(\frac{a}{W}\right)^4\right] \quad (4$$

It should be noted that Eq. (4) is the standard expression for calculation of K at the crack tip for a CT specimen. The coefficients 0.886, 4.64, –14.72, 13.32, –5.6 were used in this study. Successive crack lengths should be stored along with the corresponding cycle

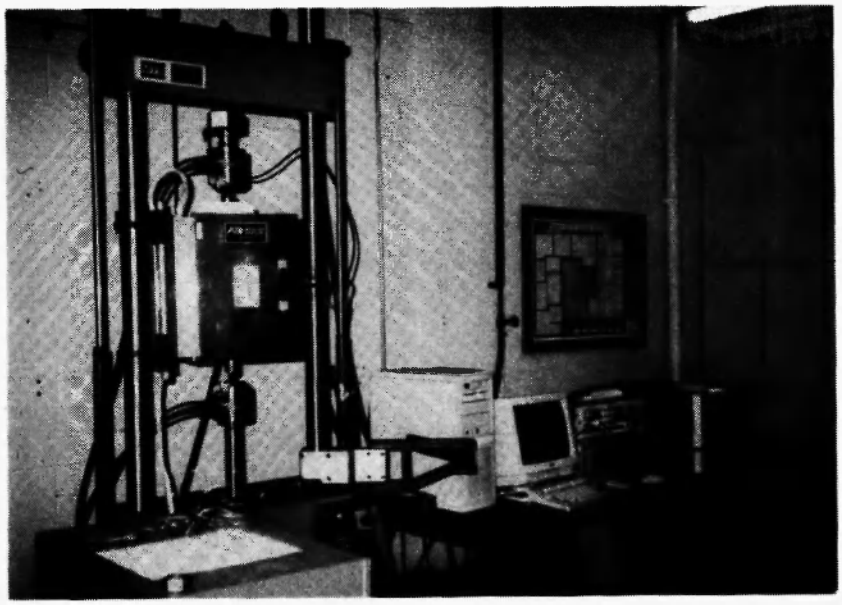

Fig. 6: Photograph of the experimental setup.

count (N), K, P_{max} and P_{min} until specimen failure. Finally, the crack growth rate da/dN is established using Eq. (5).

$$\frac{da}{dN} = \frac{(a_{i+1} - a_i)}{(N_{i+1} - N_i)} \quad (5$$

FACTORS AFFECTING ACCURACY AND QUALITY OF MEASUREMENT

Errors in crack length may arise if a blunt notch is used as the initial reference crack length, a_o /I1/. Shorter current lead spacing may also be used provided that the uniform current density requirement is not violated. If there is good consistent electrical continuity between the specimen grips and test sample, current may also be introduced directly through the gripping apparatus. In this approach the total electrical resistance through the test sample between the current input locations must be substantially less than that through the test frame to avoid a parallel circuit. For any EPD versus crack length relationships the EPD wire placement is usually a compromise between good sensitivity to crack length changes and immunity to errors caused by minor variations in lead location from sample to sample.

Lead positions near the crack tip (or notch tip locations for samples without cracks) yield better sensitivity to changes in crack length. The difficulty with this type of arrangement is that the electrical field, in general, is highly non-uniform near the crack region. Thus, minor variations in lead placement from one sample to the next may produce significant differences in the measured EPD for the same crack length /15/. In most cases, those positions which give the greatest sensitivity to crack length changes also have the greatest sensitivity to variations in lead wire positioning.

The smallest change in crack length which can be distinguished in an actual FCG test is referred to as the resolution. The resolution depends on several factors such as voltmeter resolution, amplifier gain, current magnitude, sample geometry, wire locations for voltage measurement and current input and electrical conductivity of the test material. Resolutions of better than 0.01% have been achieved for titanium. Some factors that have to be taken into consideration for maintaining accuracy and resolution will be discussed in the following paragraphs.

The DCPD method is susceptible to thermally induced electro-magnetic forces (emf), which induce potentials other than those due to the sample electrical field. Compensation for thermally induced emf is the most important consideration in minimizing crack length variability. The thermally induced voltage can be a substantial portion of the measured voltage. Since the thermally induced voltage will be present even without the current being turned on, it would be possible to account for it by subtracting voltage measurements taken with the current on with the voltage measured with the current off. An alternate method would be to take voltage measurements while reversing the direction of current flow. The corrected voltage would then be equal to one half of the difference observed at each polarity.

Changes in sample temperature can also result in false indications of crack length change or increased scatter of data. Variations in the gain of amplifiers, or the current source, can result in erroneous readings. To compensate for these effects voltage measurements can be normalized by dividing the measured voltage by a reference voltage at a location on the sample that will not be affected by crack length changes. This, however, is not feasible while employing the CT configuration.

The DCPD method requires the ability to detect small changes in DC voltage with relatively low DC signal to AC rms noise ratios. To minimize noise a combination of analog and digital filtering may be used. Digital filtering involves averaging a series of successive analog to digital conversions of the measured potential difference without restricting the response time.

Block averaging is a means of further reducing scatter in the data by averaging blocks of EPD data over one or more fatigue cycles, switching or reversing current and again averaging the signal over one or more fatigue cycles with the current in the reverse direction. This may be repeated several times before determining the average EPD response during the interval. The number of analog to digital conversions, blocks, and current switching intervals should be adjusted to minimize the crack length resolution.

Since the DCPD method relies on a current of constant magnitude flowing through the sample, it must be ensured that no portion of the supplied current is shunted in a parallel circuit through the test machine frame even though this is usually avoided in all commercial test machines. It should also be ensured that the resistance of the grips without the specimen in them should be much higher than the resistance of the sample between the current supply locations.

Careful selection of wires and modes of attachment will prevent a lot of problems associated with the DCPD method. The current supply wires should be checked for strength, melting point and also oxidation resistance while testing in corrosive environments. The current carrying ability and ease of attachment are also vital parameters to be checked. The voltage wires should be as fine as possible to allow precise fixing on the sample and also to reduce stresses so as to prevent detachment during fatigue loading. The wires may be resistance (spot) welded to the specimen to ensure a reliable joint. The voltage wires should be as short as possible and held rigid so that stray voltages owing to static fields in their surroundings should not influence the data.

The DCPD method has been demonstrated to be an extremely accurate method for crack length determination, provided that proper care and precautions have been taken. The use of proper signal filtering and post-test correction ensure reliable data with negligible scatter.

COMPUTER CONTROLLED STRESS INTENSITY GRADIENT TECHNIQUE

The standardization of the method for fatigue crack growth testing (ASTM test method for constant load amplitude FCGR above 10^{-8} m/cycle, E-647-78T), necessitates consideration of the methods available for FCGR data acquisition /8/.

The CT specimen is generally preferred for constant amplitude positive R ratio FCGR testing, primarily because its K gradient (dk/da) at small a/N values is steeper than, say, a WOL specimen. This reduces the amount of time required to generate the same da/dN vs ΔK data. Ideally, it is desirable to generate da/dN data at K gradients independent of specimen geometry. Exercising control over the K gradient allows much steeper gradients for small values of a/W, without the undesirable feature of having too steep a K gradient at the larger values of a/W associated with constant amplitude loading.

The generation of data at the appropriate K gradient provides numerous advantages such as:

- Reduction of test time.
- The da/dN - dK data can be evenly distributed without using variable da increments.
- A wide range of data may be generated without load peaking.
- The K gradient is independent of specimen geometry.

In this work, an increasing K gradient of 4 will be used in all the tests /7,8/. This will result in the load being increased in steps for crack length increments that are constant.

The hardware and software package used in the FCGR testing was supplied by Fracture Technology Associates, Bethlehem, PA /7,8/.

DESCRIPTION OF TEST EQUIPMENT AND ACCESSORIES

The test machine used for the testing was a servo hydraulic MTS machine with a capacity of 5 kips with an induction furnace of 2000°F capacity. The gripping apparatus consisted of two 4330 solid steel bars, with flat ends on one end and brackets on the other, loading pins made of 4340 steel, and brass spacers to ensure even alignment of the specimen.

The specimens used were cut from two forged Ti-6Al-4V compressor disks that were solution treated and aged (STOA). The CT specimens contained electron discharge machine notch. A total of 4 specimens were tested at each temperature range. The dimensions of the specimen conformed to ASTM E-647 specifications. Constantan thermocouple wires of 0.032 inch and 0.02 inch were used for the current supply and voltage leads respectively. The wires were resistance welded to the specimens. Fiberglass insulating sheaths were used to insulate the current and voltage leads.

SPECIMEN PREPARATION AND MOUNTING

Each specimen was cleaned using acetone solution and the fiber glass insulating sheaths were inserted over the current and voltage leads to ensure that the wires were not in contact with any part of the gripping apparatus. The specimen was mounted on the pull rods using the loading pins and the brass spacers, and even alignment of the specimen was verified. The pull rods were then mounted in the MTS machine (under stroke control) and even alignment of the pull-rods was ensured by checking for a uniform gap between the pull rods. A direct current of 3 amps and 6 volts was maintained across the specimen in al tests. The furnace was then set to the appropriate temperature and the specimen was allowed to soak for about 2 hours.

SETTING TEST PARAMETERS

All required test parameters including notch depth for pre-cracking, initial crack length for FCGR testing, maximum load, stress ratio, K-gradient, specimen thickness, and coefficients for the polynomial expression to evaluate K were entered in the FCGR test set-up. The test machine was then switched over to load control.

PRE-CRACKING

In the pre-cracking procedure, each specimen was subjected to a maximum load of 1200 lbs and at a stress ratio of 0.1. The load waveform was sinusoidal at a frequency of 20 Hz. The K-gradient was 0 and the FCGR software was set to increase load levels based on crack growth increments detected. Each specimen was allowed to pre-crack up to 0.06 inch (0.3 inch notch depth) for the pre-cracking part. All vital test parameters including the cycle count, PD versus load waveform, load, and temperature were monitored continuously.

FCGR TESTING

The actual FCGR testing was performed after the desired pre-cracking was achieved. For the actual testing each specimen was subjected to an initial sinusoidal waveform of 900 lbs maximum at a stress ratio of 0.1 and a frequency of 20 Hz. A K-gradient of 4 was used for load increments as the crack progressed. All vital test parameters like load, frequency, voltage waveform and temperature were continuously monitored throughout the test. The crack was allowed to progress till specimen failure. A data file of PD and cycle count, generated by the FCGR package as the test progressed, was stored in the data acquisition system.

POST-TEST CORRECTION

The data file of PD and load generated for each test was then corrected to account for any difference observed between optical measurements of the pre-cracked surface and the actual initial crack length used in the test. This procedure is recommended to ensure that an accurate value of the crack length is used in the regression. This correction, however, will not affect the evaluation of the coefficient '**C**' and the slope 'n'. The corrected data file was subsequently analyzed in the analysis section of the FCGR package.

DISCUSSION – 'a' versus 'N' PLOTS

The crack length, a, and cycle count, N, plots are shown in Figs. 7 to 11 for different temperature ranges. The 'a' versus 'N' plots provide a better visualization of FCGR behavior in general. For example, at 350°F, referring to Fig. 8, it is seen that each curve has an initial flat region were change in crack length is almost negligible compared with the change in N. This is typical of Region I growth, where FCGR is generally below 1e-06 inch/cycle. However, a scatter is observed with respect to the behavior of each specimen. These observations are also evident in the plots at higher temperatures. The flat region undergoes a transition that causes the curve to trace an almost vertical path gradually, where crack length changes with changes in N increasing steadily. This is typical of Region II growth where crack growth rate is steady and is between 1e-06 and 1e-03 inch/cycle. The scatter obtained in data in these plots is probably due to slight variations in microstructure of the specimens. However,

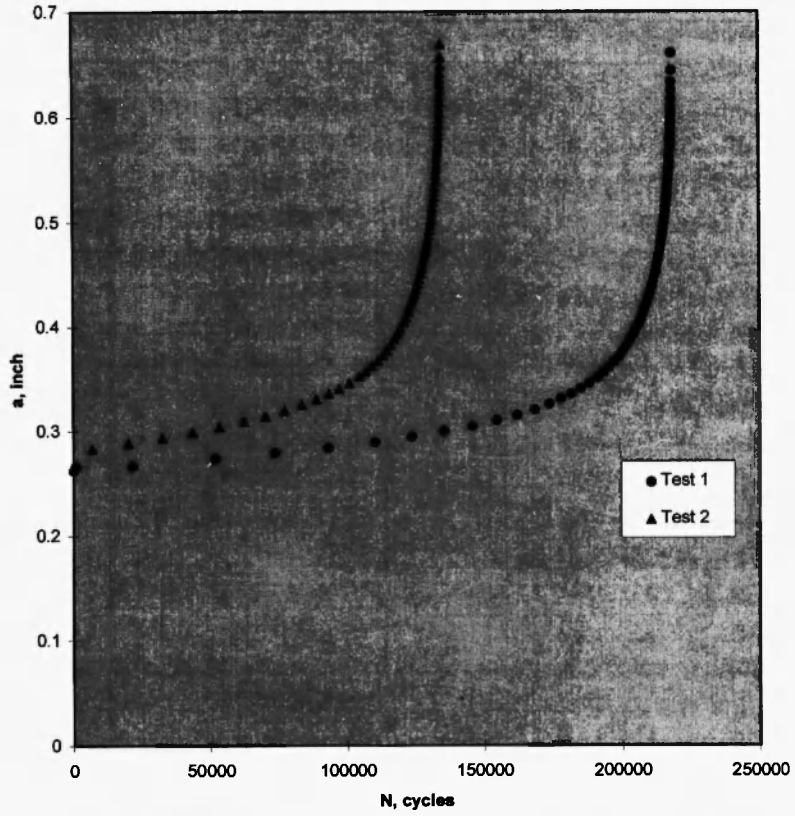

Fig. 7: Plot of a versus N of Ti-6Al-4V at room temperature.

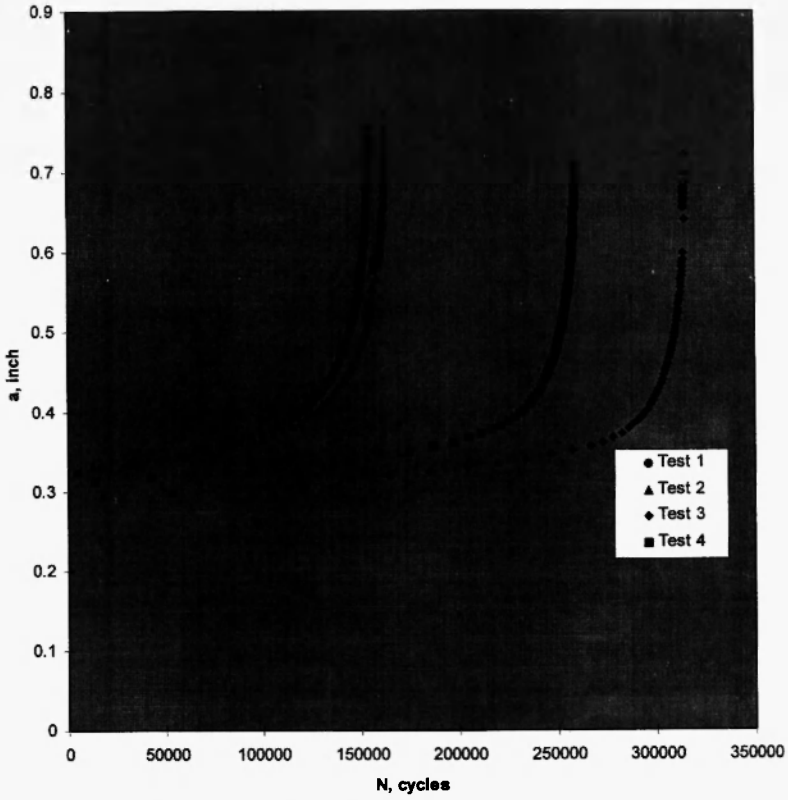

Fig. 8: Plot of a versus N of Ti-6Al-4V at 350°F.

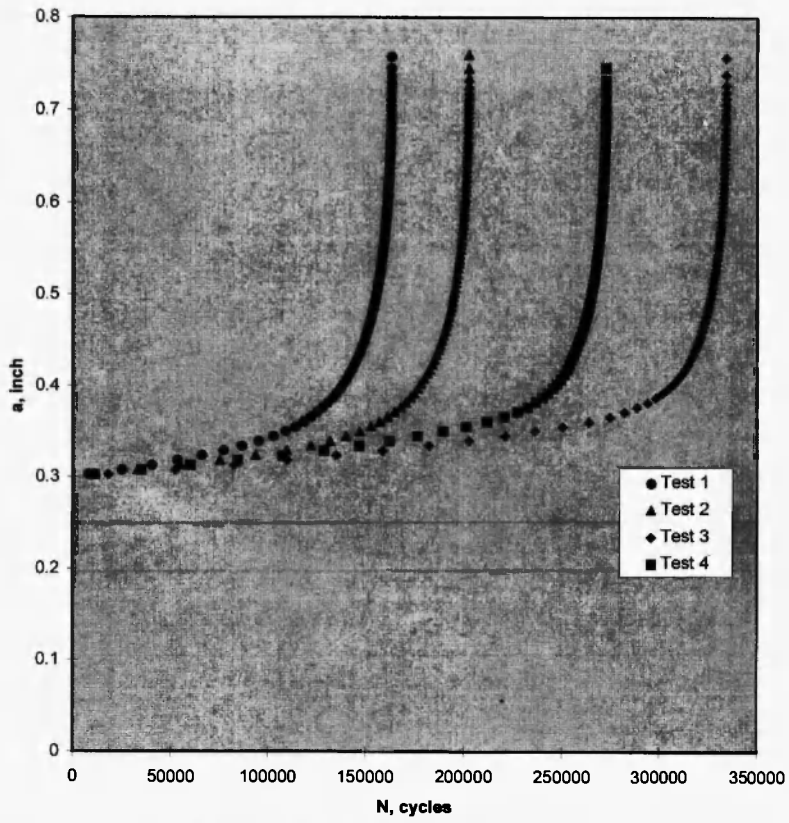

Fig. 9: Plot of a versus N of Ti-6Al-4V at 450°F.

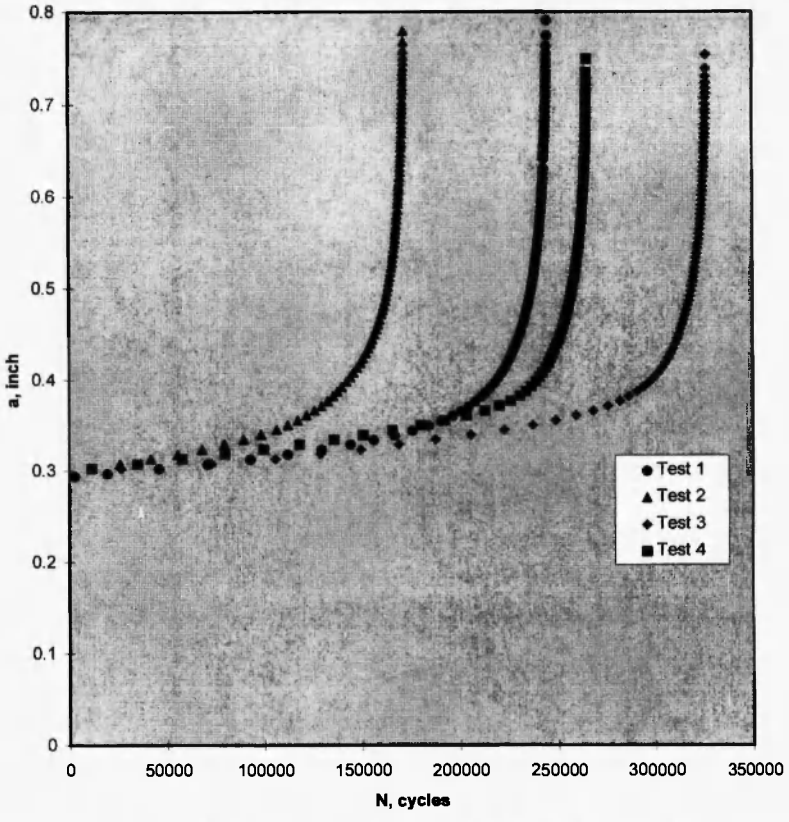

Fig. 10: Plot of a versus N of Ti-6Al-4V at 550°F.

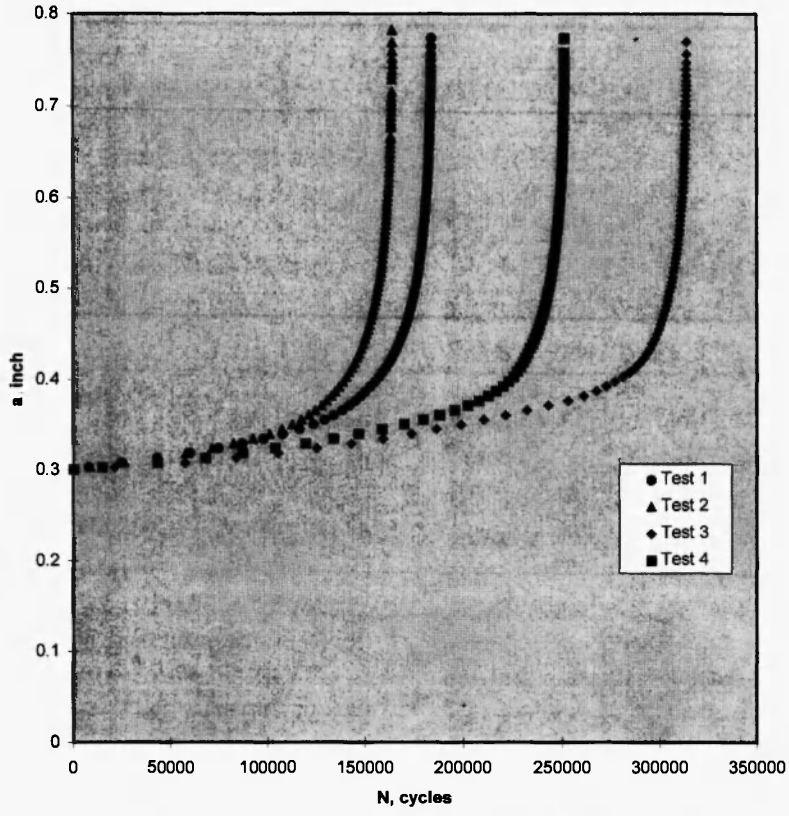

Fig. 11: Plot of a versus N of Ti-6Al-4V at 650°F.

a fractographic analysis of the specimens will reveal substantial information that could help in explaining such phenomena in subsequent papers.

CONCLUSIONS

The accuracy, ease of operation and reliability of the DCPD method in establishing FCGR was an important objective of this program. It is recommended that DCPD is a reliable method for FCGR evaluation of metals. Data obtained in this program were found to be consistent evidenced in the a-N plots and the scatter therein. This fact establishes the selection of this method over other methods for elevated temperature fatigue crack growth rate testing. More work needs to be undertaken to assess the applicability of this method with other complex cycles such as dwell conditions, materials and CT specimens.

ACKNOWLEDGMENT

This work was supported by the Federal Aviation Administration (FAA) under grant DTFA03-91-C-0044-Task A2. The authors would like to thank the program monitor Mr. Bruce Fenton at the FAA (Aviation Safety Division, Atlantic City International Airport, NJ) for the support. The authors would also like to thank Prof. Richard T. Johnson, Chair, Mechanical Engineering Department, Wichita State University, for providing the facilities to complete the work. The authors would also like to thank Dr. David Wu, Mr. Joe Adams and Dr. A. Tosoojee of Allied Signal, Engines Division, for the provision of Ti forgings and support.

REFERENCES

1. G.R. Yoder, L.A. Cooley and T.W. Crooker, *Eng. Fracture Mech.*, **11**, 805-816 (1979).
2. G.R. Yoder and D. Eylon, *Met. Trans.*, **10A**, 1808-1810 (1979).
3. R.J.H. Wanhill, R. Galatolo and C.E.W. Looije, *I.J. Fatigue*, 407-416 (1989).
4. A.J.A. Mom and M.D. Raizenne, AGARD engine disk cooperative test program, AGARD Report No. 766, 1988.
5. J. Petit, W. Berata and B. Bouchet, *Fatigue Crack Growth Behavior of Ti-6Al-4V at Elevated Temperature in High Vacuum*, Pergamon Press Ltd., 1992.
6. T. Goswami, in: *Proc. Mechanical Behavior of Materials VI*, M. Jono and T. Inoue (Eds.), Pergamon Press, 1991; 2: 59-65.
7. J.K. Donald, Fatigue crack propagation and the role of automated testing, *ASTM Standardization News*, November, 1985.
8. J.K. Donald and D.W. Schmidt, *Journal of Testing and Evaluation*, 8 (1), 19-24 (1980).
9. J.K. Donald and J. Ruschav, Direct current potential difference fatigue crack measurement techniques, EMAS Publication, 1990.
10. M.D. Raizenne, Fatigue crack growth results for Ti-6Al-4V, IMI 685 and Ti-17, Institute for Aerospace Research, National Research Council of Canada, Ontario, [[year]].
11. H.H. Johnson, *Materials Research and Standards*, 5 (9), 442-445 (1965).
12. R.H. Van Stone and T.L. Richardson, in: *Proc. ASTM STP 877 – Automated Test Methods for Fracture and Fatigue Crack Growth*, W.H. Cullen, R.W. Landgraf and J.H. Underwood (Eds.), 1985; pp. 148-166.
13. R.P. Gangloff, *Fatigue Fracture Eng. Mater. Structure*, 4, 15-33 (1981).
14. M.A. Hicks and A.C. Pickard, *I.J. Fracture*, 20, 91-101 (1982).
15. G.H. Aronson and R.O. Ritchie, *JTEVA*, 7 (4), 208-215 (1979).
16. M.R. Pishva, N.C. Bellinger, T. Terada and A.K. Koul, Laboratory Technical Report, LTR-ST-1635, National Research Council of Canada, 1987.